

Supporting Information

Separation of ethanol-water mixtures by liquid- liquid extraction using phosphonium-based ionic liquids

*Catarina M. S. S. Neves^a, José F. O. Granjo^b, Mara G. Freire^a, Al Robertson^c, Nuno M.C.
Oliveira^b and João A. P. Coutinho^{a*}*

^aCICECO, Departamento de Química, Universidade de Aveiro, 3810-193 Aveiro,
Portugal

^bCIEPQPF, Departamento de Engenharia Química, Universidade de Coimbra, 3030-790
Coimbra, Portugal

^cCytec Canada Inc., 9061 Garner Road, Niagara Falls, Ontario, Canada L2E 6S5

*Corresponding author

Tel: +351-234-370200; Fax: +351-234-370084; E-mail address: jcoutinho@ua.pt

Experimental data of the systems IL + water + EtOH

Table S1 Experimental data and critical point calculated by the Sherwood method¹ for the ternary system [TDTHP][Phosph] + H₂O + EtOH.

Phase	Mass Fraction			Selectivity (<i>S</i>)
	<i>w</i> _{IL}	<i>w</i> _{EtOH}	<i>w</i> _{H₂O}	
	0.840	0.000	0.160	
Top	0.356	0.449	0.195	1.74
Bottom	0.053	0.539	0.408	
Top	0.524	0.335	0.141	3.13
Bottom	0.001	0.432	0.567	
Top	0.620	0.255	0.125	4.39
Bottom	0.001	0.317	0.682	
Top	0.718	0.161	0.121	5.68
Bottom	0.000	0.190	0.810	
Critical Point	0.18	0.54	0.28	

Table S2 Experimental data and critical point calculated by the Sherwood method¹ for the ternary system [TDTHP][Deca] + H₂O + EtOH.

Phase	Mass Fraction			Selectivity (<i>S</i>)
	<i>w</i> _{IL}	<i>w</i> _{EtOH}	<i>w</i> _{H₂O}	
	0.851	0.000	0.149	
Top	0.392	0.419	0.189	2.00
Bottom	0.032	0.509	0.459	
Top	0.513	0.341	0.146	3.09
Bottom	0.003	0.429	0.568	
Top	0.615	0.256	0.129	4.34
Bottom	0.000	0.315	0.685	
Top	0.716	0.162	0.122	5.31
Bottom	0.000	0.201	0.799	
Critical Point	0.21	0.55	0.24	

Table S3 Experimental data and critical point calculated by the Sherwood method¹ for the ternary system [TDTHP]Cl + H₂O + EtOH.

Phase	Mass Fraction			Selectivity (<i>S</i>)
	<i>w</i> _{IL}	<i>w</i> _{EtOH}	<i>w</i> _{H₂O}	
	0.866	0.000	0.134	
Top	0.438	0.395	0.167	2.24
Bottom	0.079	0.472	0.449	
Top	0.620	0.271	0.109	5.28
Bottom	0.000	0.319	0.681	
Top	0.807	0.082	0.111	6.61
Bottom	0.000	0.100	0.900	
Top	0.723	0.175	0.102	6.97
Bottom	0.000	0.198	0.802	
Critical Point	0.25	0.49	0.26	

Table S4 Experimental data and critical point calculated by the Sherwood method¹ for the ternary system [TDTHP][CH₃SO₃] + H₂O + EtOH.

Phase	Mass Fraction			Selectivity (<i>S</i>)
	<i>w</i> _{IL}	<i>w</i> _{EtOH}	<i>w</i> _{H₂O}	
	0.872	0.000	0.128	
Top	0.590	0.257	0.153	2.29
Bottom	0.031	0.306	0.663	
Top	0.703	0.176	0.121	3.64
Bottom	0.006	0.218	0.776	
Top	0.510	0.305	0.185	5.18
Bottom	0.088	0.381	0.531	
Top	0.795	0.085	0.120	6.67
Bottom	0.004	0.096	0.900	
Critical Point	0.40	0.37	0.23	

Table S5 Experimental data and critical point calculated by the Sherwood method¹ for the ternary system [TDTHP]Br + H₂O + EtOH.

Phase	Mass Fraction			Selectivity (<i>S</i>)
	<i>w</i> _{IL}	<i>w</i> _{EtOH}	<i>w</i> _{H₂O}	
	0.932	0.000	0.068	
Top	0.128	0.572	0.300	0.566
Bottom	0.448	0.426	0.126	
Top	0.054	0.555	0.391	2.74
Bottom	0.562	0.348	0.090	
Top	0.645	0.280	0.075	4.73
Bottom	0.010	0.436	0.554	
Top	0.718	0.223	0.059	7.76
Bottom	0.001	0.326	0.673	
Critical Point	0.28	0.53	0.19	

Table S6 Experimental data and critical point calculated by the Sherwood method¹ for the ternary system [TDTHP][N(CN)₂] + H₂O + EtOH.

Phase	Mass Fraction			Selectivity (<i>S</i>)
	<i>w</i> _{IL}	<i>w</i> _{EtOH}	<i>w</i> _{H₂O}	
	0.967	0.000	0.033	
Top	0.434	0.458	0.108	1.69
Bottom	0.114	0.634	0.252	
Top	0.622	0.313	0.065	3.41
Bottom	0.020	0.574	0.406	
Top	0.712	0.238	0.050	5.48
Bottom	0.009	0.463	0.528	
Top	0.787	0.169	0.044	7.76
Bottom	0.008	0.330	0.662	
Critical Point	0.28	0.16	0.56	

Table S7 Experimental data and critical point calculated by the Sherwood method¹ for the ternary system [TDTHP][NTf₂] + H₂O + EtOH.

Phase	Mass Fraction			Selectivity (<i>S</i>)
	<i>w</i> _{IL}	<i>w</i> _{EtOH}	<i>w</i> _{H₂O}	
	0.998	0.000	0.002	
	0.384	0.553	0.063	
	0.318	0.612	0.070	
	0.272	0.652	0.076	
	0.235	0.686	0.079	
	0.210	0.707	0.083	
	0.189	0.727	0.084	
	0.174	0.738	0.088	
	0.160	0.752	0.088	
	0.153	0.754	0.093	
	0.141	0.766	0.093	
	0.135	0.767	0.098	
	0.041	0.765	0.193	
	0.176	0.741	0.083	
	0.222	0.702	0.076	
	0.244	0.684	0.072	
	0.263	0.668	0.069	
	0.281	0.652	0.067	
	0.297	0.638	0.065	
	0.470	0.048	0.482	
Top	0.090	0.788	0.122	2.57
Bottom	0.848	0.144	0.008	
Top	0.012	0.737	0.251	4.16
Bottom	0.937	0.058	0.005	
Top	0.001	0.605	0.394	6.12
Bottom	0.955	0.041	0.004	
Top	0.000	0.485	0.515	11.31
Bottom	0.964	0.033	0.003	
Top	0.000	0.226	0.774	21.66
Bottom	0.983	0.015	0.002	
Critical Point	0.73	0.26	0.01	

Table S8 Absolute deviations between experimental data and NRTL correlated data of the ternary system [TDTHP][Phosph] + H₂O + EtOH.

IL	Phase	Experimental data			NRTL correlated data			Absolute Deviation ($ w_{\text{exp}} - w_{\text{NRTL}} $)		
		w_{IL}	w_{EtOH}	$w_{\text{H}_2\text{O}}$	w_{IL}	w_{EtOH}	$w_{\text{H}_2\text{O}}$	w_{IL}	w_{EtOH}	$w_{\text{H}_2\text{O}}$
[TDTHP][Phosph]		0.840	0.000	0.160	0.842	0.000	0.158	0.002	0.000	0.002
	Top	0.356	0.449	0.195	0.363	0.437	0.200	0.007	0.012	0.005
	Bottom	0.053	0.539	0.408	0.059	0.542	0.399	0.006	0.003	0.009
	Top	0.524	0.335	0.141	0.519	0.330	0.151	0.005	0.005	0.010
	Bottom	0.001	0.432	0.567	0.007	0.427	0.567	0.006	0.005	0.000
	Top	0.621	0.255	0.125	0.614	0.259	0.128	0.007	0.004	0.003
	Bottom	0.001	0.317	0.682	0.001	0.313	0.686	0.000	0.005	0.004
	Top	0.718	0.161	0.121	0.718	0.173	0.109	0.000	0.012	0.012
	Bottom	0.000	0.190	0.810	0.000	0.186	0.814	0.000	0.004	0.004

Table S9 Absolute deviations between experimental data and NRTL correlated data of the ternary system [TDTHP][Deca] + H₂O + EtOH.

IL	Phase	Experimental data			NRTL correlated data			Absolute Deviation ($ w_{\text{exp}} - w_{\text{NRTL}} $)		
		w_{IL}	w_{EtOH}	$w_{\text{H}_2\text{O}}$	w_{IL}	w_{EtOH}	$w_{\text{H}_2\text{O}}$	w_{IL}	w_{EtOH}	$w_{\text{H}_2\text{O}}$
[TDTHP][Deca]		0.851	0.000	0.149	0.855	0.000	0.146	0.003	0.000	0.003
	Top	0.512	0.341	0.146	0.508	0.335	0.157	0.005	0.006	0.011
	Bottom	0.004	0.429	0.568	0.009	0.424	0.567	0.005	0.005	0.001
	Top	0.615	0.256	0.129	0.610	0.259	0.131	0.005	0.003	0.002
	Bottom	0.000	0.315	0.685	0.001	0.311	0.688	0.001	0.004	0.003
	Top	0.716	0.163	0.122	0.710	0.177	0.113	0.005	0.014	0.009
	Bottom	0.000	0.201	0.799	0.000	0.194	0.806	0.000	0.007	0.007
	Top	0.392	0.419	0.189	0.400	0.409	0.191	0.008	0.010	0.003
	Bottom	0.031	0.509	0.459	0.040	0.510	0.450	0.009	0.001	0.009

Table S10 Absolute deviations between experimental data and NRTL correlated data of the ternary system [TDTHP]Cl + H₂O + EtOH.

IL	Phase	Experimental data			NRTL correlated data			Absolute Deviation ($ w_{\text{exp}} - w_{\text{NRTL}} $)		
		w_{IL}	w_{EtOH}	$w_{\text{H}_2\text{O}}$	w_{IL}	w_{EtOH}	$w_{\text{H}_2\text{O}}$	w_{IL}	w_{EtOH}	$w_{\text{H}_2\text{O}}$
[TDTHP]Cl		0.866	0.000	0.134	0.861	0.001	0.138	0.005	0.001	0.004
	Top	0.438	0.395	0.168	0.429	0.387	0.184	0.008	0.008	0.017
	Bottom	0.079	0.472	0.449	0.058	0.488	0.455	0.021	0.016	0.006
	Top	0.620	0.271	0.109	0.623	0.254	0.123	0.003	0.017	0.014
	Bottom	0.000	0.319	0.681	0.005	0.322	0.674	0.005	0.003	0.007
	Top	0.723	0.175	0.102	0.729	0.170	0.101	0.006	0.005	0.001
	Bottom	0.000	0.198	0.802	0.000	0.202	0.798	0.000	0.004	0.004
	Top	0.807	0.082	0.111	0.815	0.091	0.094	0.007	0.009	0.017
	Bottom	0.000	0.100	0.900	0.000	0.099	0.901	0.000	0.002	0.001

Table S11 Absolute deviations between experimental data and NRTL correlated data of the ternary system [TDTHP][CH₃SO₃] + H₂O + EtOH.

IL	Phase	Experimental data			NRTL correlated data			Absolute Deviation ($ w_{\text{exp}} - w_{\text{NRTL}} $)		
		w_{IL}	w_{EtOH}	$w_{\text{H}_2\text{O}}$	w_{IL}	w_{EtOH}	$w_{\text{H}_2\text{O}}$	w_{IL}	w_{EtOH}	$w_{\text{H}_2\text{O}}$
[TDTHP][CH ₃ SO ₃]		0.872	0.000	0.128	0.881	0.000	0.119	0.009	0.000	0.009
	Top	0.590	0.257	0.153	0.597	0.245	0.158	0.007	0.013	0.005
	Bottom	0.031	0.306	0.663	0.034	0.311	0.655	0.002	0.005	0.008
	Top	0.703	0.176	0.121	0.695	0.171	0.135	0.008	0.005	0.013
	Bottom	0.006	0.218	0.776	0.019	0.208	0.774	0.012	0.010	0.002
	Top	0.510	0.305	0.185	0.504	0.308	0.188	0.006	0.003	0.003
	Bottom	0.088	0.381	0.531	0.067	0.395	0.538	0.021	0.014	0.007
	Top	0.795	0.085	0.120	0.798	0.083	0.119	0.002	0.002	0.001
	Bottom	0.003	0.092	0.905	0.013	0.093	0.894	0.009	0.001	0.010

Table S12 Absolute deviations between experimental data and NRTL correlated data of the ternary system [TDTHP]Br + H₂O + EtOH.

IL	Phase	Experimental data			NRTL correlated data			Absolute Deviation ($ w_{\text{exp}} - w_{\text{NRTL}} $)		
		w_{IL}	w_{EtOH}	$w_{\text{H}_2\text{O}}$	w_{IL}	w_{EtOH}	$w_{\text{H}_2\text{O}}$	w_{IL}	w_{EtOH}	$w_{\text{H}_2\text{O}}$
[TDTHP]Br		0.937	0.000	0.063	0.934	0.000	0.066	0.003	0.000	0.003
	Top	0.054	0.555	0.391	0.047	0.555	0.398	0.007	0.000	0.007
	Bottom	0.562	0.348	0.090	0.551	0.346	0.103	0.012	0.002	0.013
	Top	0.645	0.280	0.075	0.649	0.273	0.078	0.004	0.007	0.003
	Bottom	0.010	0.436	0.554	0.007	0.440	0.553	0.003	0.004	0.001
	Top	0.128	0.572	0.300	0.129	0.579	0.292	0.000	0.007	0.008
	Bottom	0.449	0.426	0.126	0.451	0.418	0.132	0.002	0.008	0.006
	Top	0.718	0.223	0.059	0.718	0.220	0.062	0.000	0.003	0.003
	Bottom	0.001	0.326	0.673	0.001	0.326	0.673	0.000	0.001	0.000

Table S13 Absolute deviations between experimental data and NRTL correlated data of the ternary system [TDTHP][N(CN)₂] + H₂O + EtOH.

IL	Phase	Experimental data			NRTL correlated data			Absolute Deviation ($ w_{\text{exp}} - w_{\text{NRTL}} $)		
		w_{IL}	w_{EtOH}	$w_{\text{H}_2\text{O}}$	w_{IL}	w_{EtOH}	$w_{\text{H}_2\text{O}}$	w_{IL}	w_{EtOH}	$w_{\text{H}_2\text{O}}$
[TDTHP][N(CN) ₂]		0.967	0.000	0.033	0.978	0.009	0.013	0.011	0.009	0.021
	Top	0.622	0.313	0.065	0.623	0.311	0.067	0.001	0.003	0.002
	Bottom	0.020	0.574	0.406	0.021	0.574	0.405	0.001	0.000	0.001
	Top	0.712	0.238	0.050	0.689	0.256	0.054	0.023	0.018	0.005
	Bottom	0.009	0.463	0.528	0.003	0.457	0.539	0.006	0.006	0.011
	Top	0.434	0.458	0.108	0.462	0.437	0.102	0.028	0.021	0.006
	Bottom	0.115	0.634	0.252	0.144	0.626	0.230	0.029	0.008	0.022
	Top	0.787	0.169	0.044	0.753	0.204	0.043	0.034	0.035	0.001
	Bottom	0.009	0.330	0.662	0.000	0.318	0.681	0.008	0.011	0.020

Table S14 Absolute deviations between experimental data and NRTL correlated data of the ternary system [TDTHP][NTf₂] + H₂O + EtOH.

IL	Phase	Experimental data			NRTL correlated data			Absolute Deviation ($ w_{\text{exp}} - w_{\text{NRTL}} $)		
		w_{IL}	w_{EtOH}	$w_{\text{H}_2\text{O}}$	w_{IL}	w_{EtOH}	$w_{\text{H}_2\text{O}}$	w_{IL}	w_{EtOH}	$w_{\text{H}_2\text{O}}$
[TDTHP][NTf ₂]		0.998	0.000	0.002	0.999	0.000	0.001	0.001	0.000	0.001
	Top	0.012	0.737	0.252	0.049	0.697	0.254	0.037	0.039	0.002
	Bottom	0.937	0.058	0.005	0.903	0.090	0.007	0.034	0.032	0.002
	Top	0.090	0.789	0.122	0.152	0.735	0.114	0.062	0.054	0.008
	Bottom	0.848	0.144	0.009	0.864	0.128	0.008	0.017	0.016	0.001
	Top	0.000	0.485	0.515	0.005	0.480	0.515	0.005	0.005	0.000
	Bottom	0.964	0.033	0.003	0.930	0.065	0.005	0.035	0.032	0.002
	Top	0.001	0.605	0.394	0.015	0.593	0.392	0.014	0.012	0.002
	Bottom	0.955	0.041	0.004	0.920	0.074	0.006	0.035	0.033	0.002
	Top	0.000	0.226	0.774	0.000	0.222	0.778	0.000	0.004	0.004
	Bottom	0.983	0.015	0.002	0.954	0.043	0.003	0.029	0.028	0.001

Comparison between all experimental ternary phase diagrams

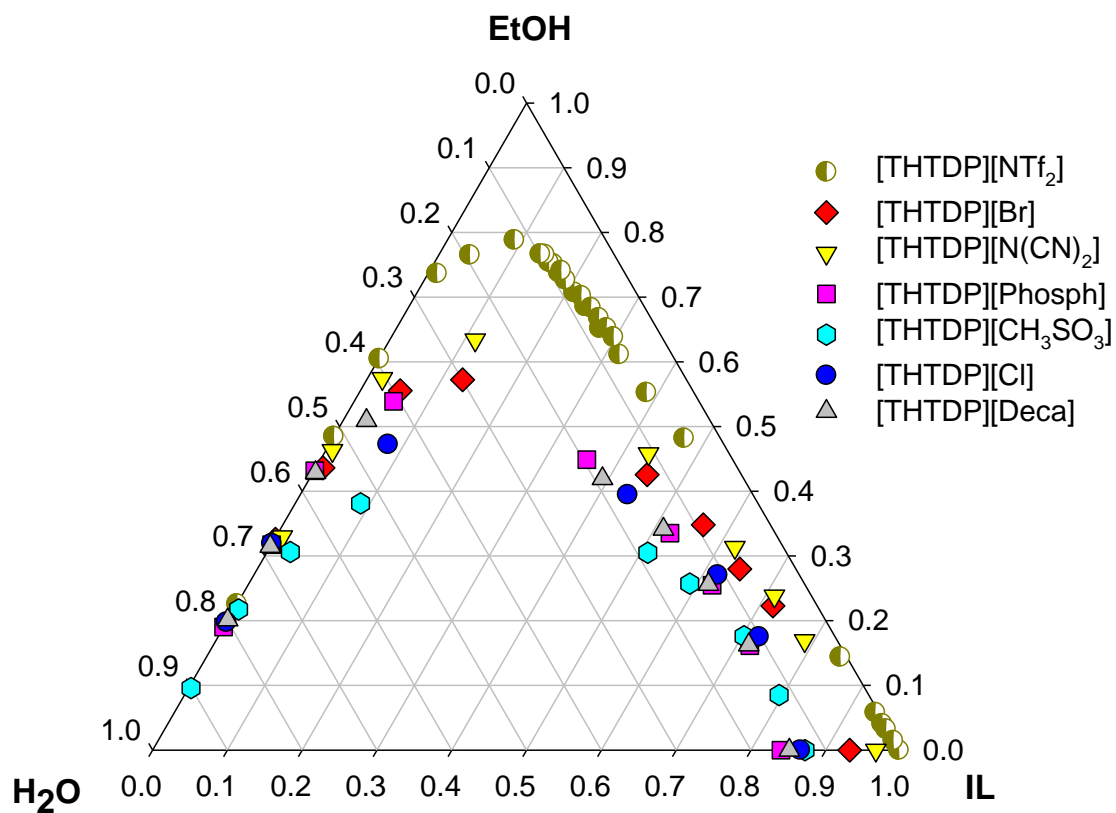


Fig. S1 Experimental ternary phase diagrams for all IL + EtOH + H₂O systems at 298.15 K (mass fraction units).

Consistency of the experimental tie-lines

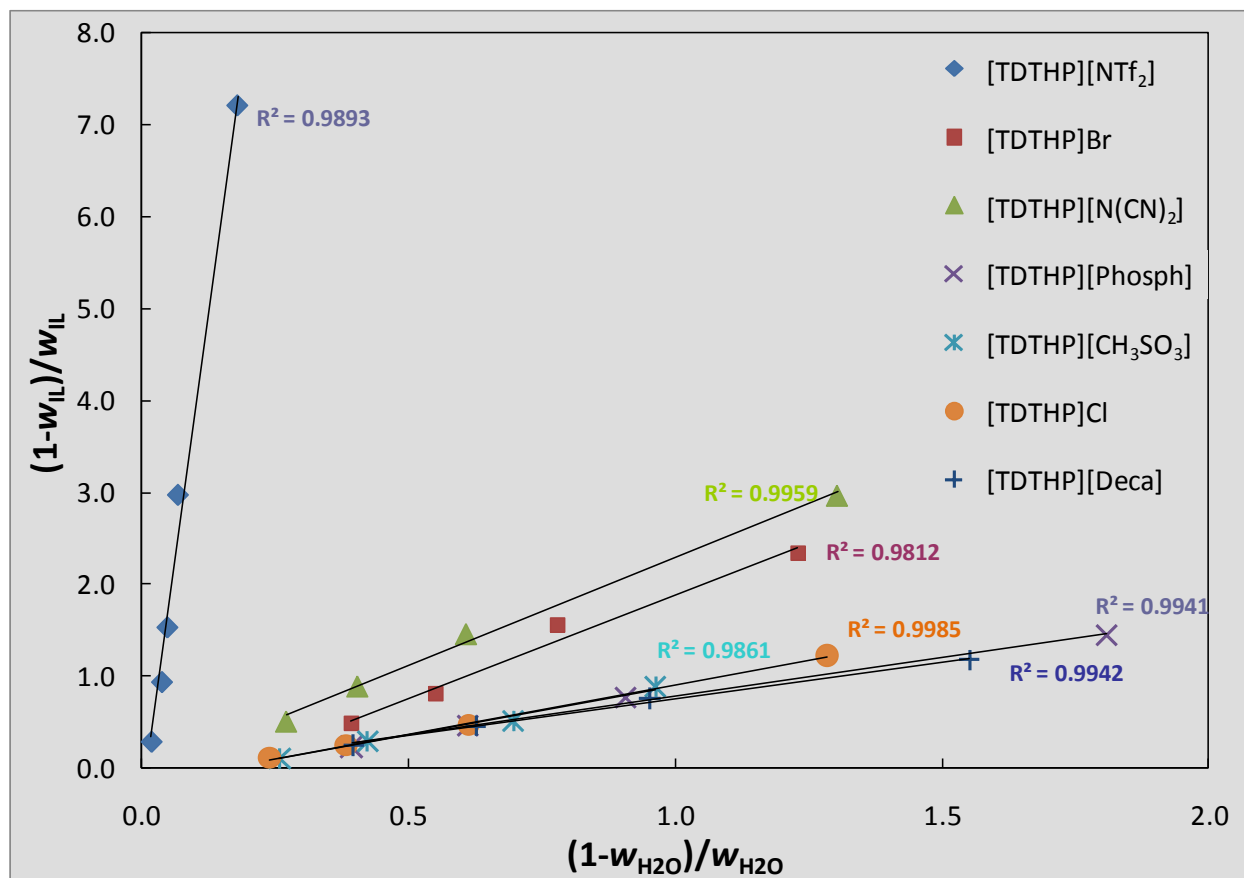


Fig. S2 Tie-Lines correlation using the Othmer-Tobias correlation² for each ternary system IL + EtOH + Water.

***S* and *D* dependence on the ethanol content**

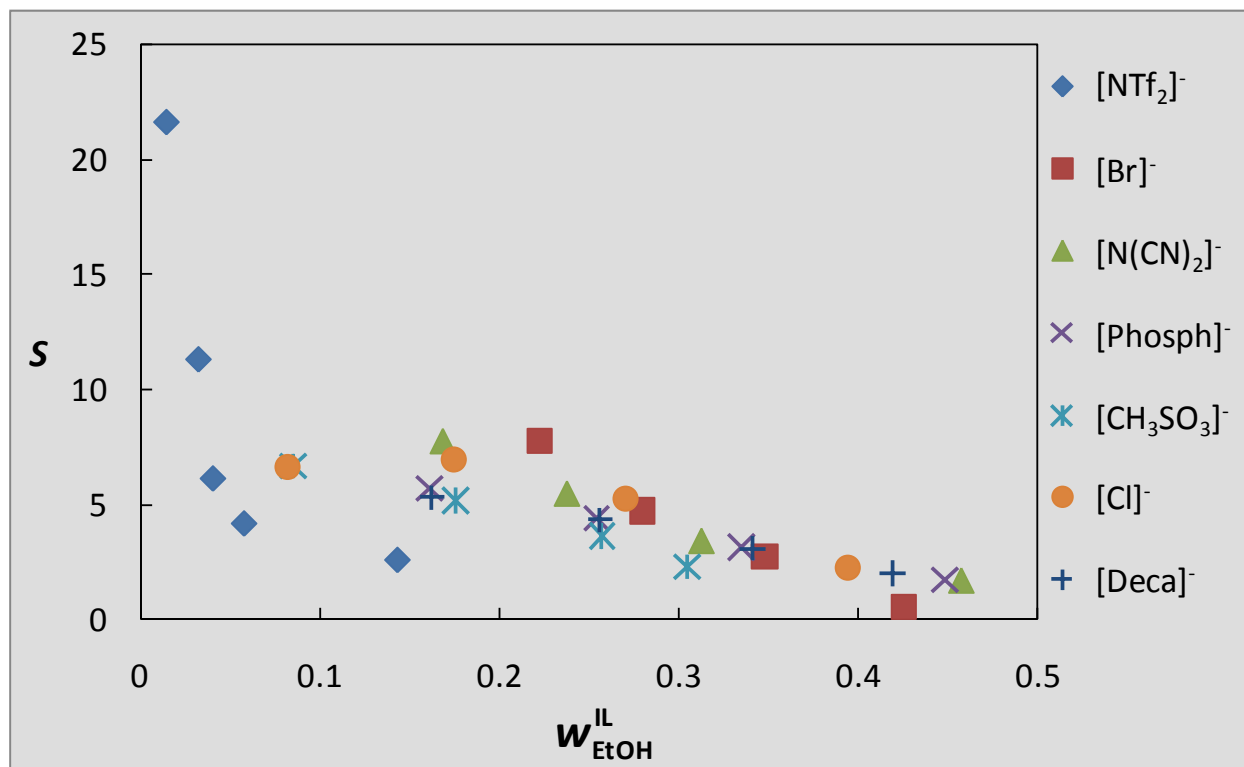


Fig. S3 Correlation of ethanol selectivities (*S*) as a function of the ethanol content in the ionic liquid rich-phase ($w_{\text{EtOH}}^{\text{IL}}$).

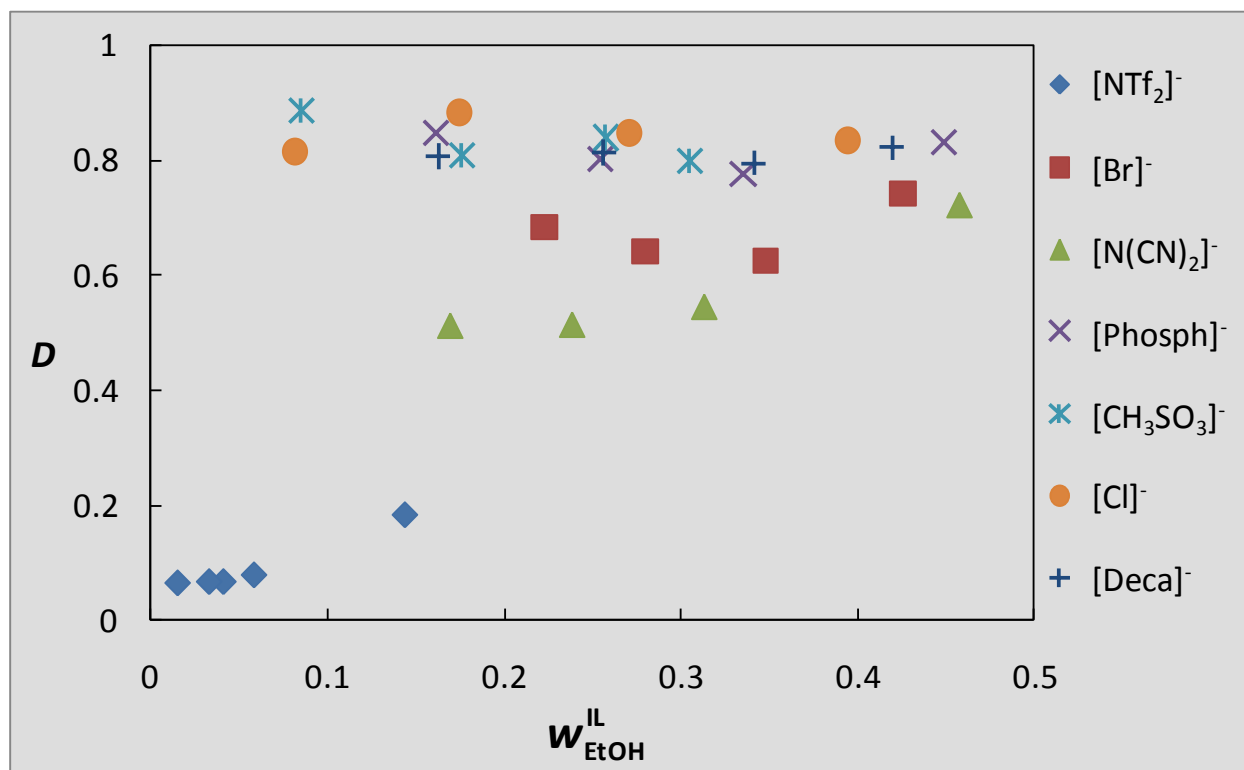


Fig. S4 Correlation of ethanol distribution coefficients (D) as a function of the ethanol content in the ionic liquid rich-phase ($w_{\text{EtOH}}^{\text{IL}}$).

NRTL parameter estimation

The expressions for the excess Gibbs energy (g^E) and the logarithm of the activity coefficient ($\ln \gamma_i$) given by the NRTL model can be written as³:

$$\frac{g^E}{RT} = \sum_i^{n_c} x_i \ln \gamma_i = \sum_i^{n_c} \frac{x_i L_i}{M_i} \quad (\text{S1})$$

$$\ln \gamma_i = \frac{L_i}{M_i} + \sum_j^{n_c} \frac{x_j G_{ij}}{M_j} \left(\tau_{ij} - \frac{L_j}{M_j} \right) \quad (\text{S2})$$

$$L_i = \sum_k^{n_c} x_k \tau_{ki} G_{ki} \quad (\text{S3})$$

$$M_i = \sum_k^{n_c} x_k G_{ki} \quad (\text{S4})$$

$$G_{ij} = e^{-\alpha_{ij} \tau_{ij}} \quad (\text{S5})$$

$$\tau_{ij} = \frac{(g_{ij} - g_{ii})}{RT} = \frac{\Delta g_{ij}}{RT}, \quad i \neq j \text{ and } \tau_{ij} = 0, \quad i = j \quad (\text{S6})$$

Here $i, j, k \in \{1, 2, 3\}$ represent the different molecular species in the mixture (1 – water, 2 – ethanol, 3 – IL), n_c is the number of components, and x_i refers to molar fractions. In the present work, the parameter estimation task was formulated as the solution of a nonlinear programming problem (NLP), using the weighted norm of the differences between the experimental mass fractions and the values predicted by the model as an objective function⁴:

$$\min_z \phi = \sum_i^{n_t} \sum_j^{n_c} \sum_k^2 \omega_{ijk} e_{ijk}(\tau)^2$$

where $e_{ijk}(\tau) = w_{ijk}^{\text{exp}} - w_{ijk}^{\text{mod}}(\tau)$, and the superscripts *exp* and *mod* correspond to experimental and predicted mass fraction values, respectively. The summations in this equation are taken over all tie-lines (*i*), components (*j*) and phases (*k*), and ω_{ijk} is a weight factor associated with each error term. Using the isothermal data available for each system, the objective function ϕ was minimized by simultaneous determination of all model variables (here denoted as *z*), subject to constraints of iso-activity, the NRTL activity model described by equations (S2-S6), sum of mass and molar fraction restrictions, and magnitude bounds for the model parameters τ_{ij} . Mass fractions were used in the data regression, due to the large differences in molecular weights between the ILs and the molecular components.

To address the non-convexity of this nonlinear parameter estimation problem, which often leads to multiple local optimal solutions, this problem was implemented in GAMS⁵, taking advantage of the robustness of the numerical solvers available in this system. Additionally, considerable care was placed in the reformulation of the original model equations, as NLP constraints. This was done by introducing new terms and using algebraic rearrangements in the resultant equations that allowed the nonlinearity of each individual component of the model to be significantly decreased. Scaling of the resulting variables and equations was performed, also with the purpose of reducing the overall model nonlinearity. A subset of fundamental model variables was identified, and proper initialization and bounds were established for them. These values were then propagated throughout the model to initialize and bound the remaining variables, allowing both a more consistent global model initialization, and avoiding the nonconvergence of the NLP due to the inability of locating feasible solutions. This step was verified to be an

essential task to guarantee the convergence of the parameter estimation. The following numerical solvers were used in this study:

- CONOPT⁶ – based on the General Reduced Gradient and Successive Quadratic Programming algorithms; provides a very robust initialization and location of feasible points in highly constrained problems; suitable for medium to large scale NLPs;
- OQNLP⁷ – a global solver based on various heuristic multistart algorithms; designated to rapidly finding various local optima of smooth constrained NLPs;
- BARON⁸ – a global numerical solver for continuous and discrete variables; based on a deterministic global optimization algorithm; capable of determining and refining model bounds in different regions of the solution domain.

Each of these solvers was tested with each LLE ternary system, to ensure that the set of parameters obtained corresponds to the best possible solutions using this type of formulation. The values of the residual function ϕ at the optimum were comprised between 0.7×10^{-3} (system with Br^-) and 7×10^{-3} (for the system with $[\text{N}(\text{CN})_2]^-$). This was possible through the extensive search for alternative solutions (especially with the OQNLP solver) and by increasing the bounds allowed for the τ_{ij} parameters, which in various cases resulted in higher values for the interaction parameter τ_{13} (water – IL). This step should be interpreted with caution, since it corresponds to larger values of the respective Δg_{ij} interaction term, and would perhaps benefit from additional confirmation provided by including in the regression experimental data obtained at different temperatures.

The computer requirements for the parameter estimation task were of the order of one second of CPU, using GAMS/CONOPT on a current Intel Xeon Linux workstation. Due to different nature of the algorithms, a maximum of 30 minutes of CPU were allowed for the runs with the OQNLP solver, and 60 minutes for BARON. Within the time allowed and for all the systems considered, BARON was unable to find a guaranteed global solution, stopping often at a local solution. On the other hand, the OQNLP solver was able to identify several distinct local solutions of the problems. This number of local optima found varied from 5 (for the system with [NTf₂]) to 77 (system with Br⁻), and corresponded typically to approximately 20 different local optima, in most of the cases considered. Within this set, the solutions provided by CONOPT corresponded typically to the best (or second best) local solutions known for each problem, after reasonable tuning of the initialization scheme. From an overall perspective, the experience acquired in this part of the work indicates that the critical steps in this parameter estimation task were the proper construction of the NLP (through reformulation, scaling, initialization and bounding of the original mathematical model), and the availability of a multistart optimizer, capable of largely eliminating the effects of the initial estimates on the quality of the solutions obtained.

References

1. J. D. Seader and E. J. Henley, in *Separation Process Principles*, John Wiley & Sons, New York edn., 1998.
2. D. Othmer and P. Tobias, *Ind. Eng. Chem.*, 1942, **34**, 693-696.
3. J. P. O'Connell and J. M. Haile, in *Thermodynamics: Fundamentals for Applications*, Cambridge University Press, New York edn., 2005.
4. J. M. Sørensen, T. Magnussen, P. Rasmussen and A. Fredenslund, *Fluid Phase Equilib.*, 1979, **3**, 47-82.
5. A. Brooke, D. Ketndrick, A. Meeraus and R. Raman, in *GAMS - A User's Guide*, GAMS Development Corporation, Washington DC edn., 2005.
6. A. S. Drud, *ORSA J. Comput.*, 1992, **6**, 207-216.
7. <http://www.gams.com/dd/docs/solvers/oqnlp.pdf>, Accessed December 3rd, 2010.
8. M. Tawarmalani and N. V. Sahinidis, in *Convexification and Global Optimization in Continuous and Mixed-Integer Nonlinear Programming*, Kluwer Academic Publishers, Dordrecht edn., 2002.